

Dynamic interaction of BiP and ER stress transducers in the unfolded-protein response

Anne Bertolotti*, Yuhong Zhang*, Linda M. Hendershot* †, Heather P. Harding* and David Ron* ‡

*Skirball Institute of Biomolecular Medicine, Departments of Medicine and Cell Biology and the Kaplan Cancer Center, New York University School of Medicine, New York, New York 10016, USA

†Department of Tumour Cell Biology, St Jude Children's Research Hospital, Memphis, Tennessee 38105, USA

‡e-mail: ron@saturn.med.nyu.edu

PERK and IRE1 are type-I transmembrane protein kinases that reside in the endoplasmic reticulum (ER) and transmit stress signals in response to perturbation of protein folding. Here we show that the luminal domains of these two proteins are functionally interchangeable in mediating an ER stress response and that, in unstressed cells, both luminal domains form a stable complex with the ER chaperone BiP. Perturbation of protein folding promotes reversible dissociation of BiP from the luminal domains of PERK and IRE1. Loss of BiP correlates with the formation of high-molecular-mass complexes of activated PERK or IRE1, and overexpression of BiP attenuates their activation. These findings are consistent with a model in which BiP represses signalling through PERK and IRE1 and protein misfolding relieves this repression by effecting the release of BiP from the PERK and IRE1 luminal domains.

Conditions that alter protein folding in the ER elicit two principal cellular responses. The first involves upregulation of genes encoding chaperones and other proteins that prevent polypeptide aggregation and participate in polypeptide folding, post-translational assembly of protein complexes and protein degradation¹. The second consists of a transient attenuation in rates of protein synthesis². Both responses minimize the accumulation and aggregation of misfolded proteins, the first by increasing the capacity of the machinery for folding and degradation and the second by reducing the burden placed on them. Two ER-resident proteins are thought to have an important function in transducing the stress signal initiated by misfolded proteins to the afore-mentioned downstream effects.

In yeast, activation of gene expression by the unfolded-protein response (UPR) is dependent on the function of a type-I transmembrane protein kinase, IRE1, which resides in the ER. The luminal domain of IRE1 is thought to respond to an ER stress signal that induces oligomerization of the protein, transphosphorylation by its kinase domain, activation of its effector functions and subsequent down-stream signalling to the transcriptional apparatus^{3,4}. However, the nature of the luminal signal that activates IRE1 is unknown. Two mammalian homologues of IRE1 have been identified and found to have a similar function in ER stress signalling^{5,6}. A second transmembrane ER stress-signal transducer has also been identified. PKR-like ER kinase (PERK, also known as PEK⁷), is conserved in all known metazoans and seems to respond to a similar set of signals to those that influence IRE1, using an apparently related ER-luminal domain⁸. PERK is also a protein serine/threonine kinase that undergoes transphosphorylation in response to ER stress. Activated PERK phosphorylates the α -subunit of translation-initiation factor 2 (eIF2 α), which results in inhibition of translation initiation⁸. Thus, these two stress-response mechanisms in the ER use proteins with similar topology and similar overall organization of domains to respond to a luminal signal or signals, the nature of which is the focus of this study.

Results

Association of BiP with PERK and IRE1. To identify the proteins that interact with the luminal domains of ER stress-signal trans-

ducers and that may therefore participate in signalling, we began our studies with PERK, for which an enriched source was found in the pancreas⁷. We used an antiserum against the carboxy-terminal portion of PERK to co-immunopurify associated cellular proteins in lysates of the pancreatic acinar cell line AR42J. PERK co-purified with a cellular protein of relative molecular mass 70,000 (M_r 70K) that was absent from control immunoprecipitation reactions carried out using antisera against GCN2, a related eIF2 α kinase, or ribophorin-1, a transmembrane protein abundantly present in the ER (Fig. 1a). The protein of M_r 70K was indistinguishable in size from the ER chaperone BiP, which we immunoprecipitated using a specific anti-BiP serum (Fig. 1a). BiP is allosterically regulated by nucleotide binding, and complexes between BiP and target proteins

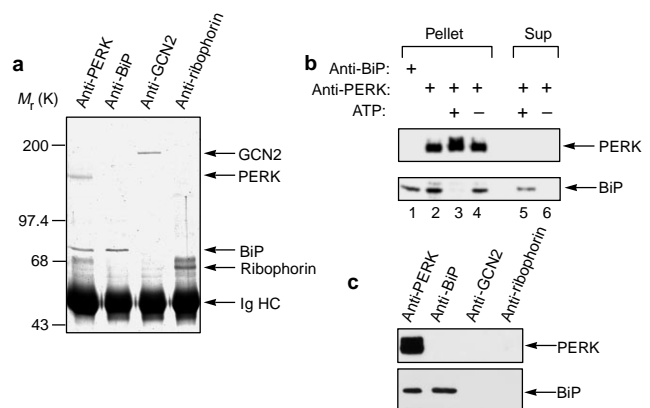


Figure 1 PERK forms a complex with BiP in unstressed cells. **a**, Stained gel of proteins immunopurified from AR42J cells, using the indicated antisera. Proteins were resolved by SDS-PAGE and stained with Coomassie blue. Ig HC, immunoglobulin heavy chain. **b**, Autoradiogram showing the proteins retained in the PERK immune complex (pellet) or released into the supernatant (sup) following incubation of the immunoprecipitates *in vitro* for 30 min at 25 °C, in the presence (+) or absence (-) of 2 mM ATP. **c**, Immunoblots, after immunoprecipitation with the indicated antisera.

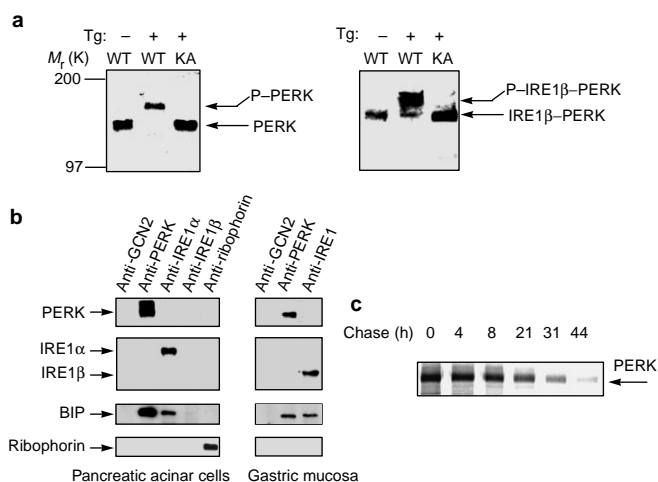


Figure 2 Functional similarities of the luminal domains of PERK and IRE1. **a**, Immunoblots against PERK from lysates of COS-1 cells transfected with the indicated expression vectors in the absence (-) or presence (+) of 1 μ M thapsigargin (Tg). WT, wild type; KA, K618A mutant lacking PERK kinase activity; P-PERK, phosphorylated PERK. The signal from endogenous PERK is not observed at the exposure shown here. **b**, Immunoblots of proteins from the pancreatic acinar cells (AR42J) or the gastric mucosa of mice. **c**, Autoradiogram showing the half-life of PERK in metabolically labelled AR42J cells. PERK was immunoprecipitated from cells labelled by a brief pulse of [³⁵S]methionine-cysteine and chased in unlabelled media for the indicated time periods.

can be disrupted by incubation *in vitro* with ATP^{9,10}. We therefore incubated PERK-containing complexes immunopurified from metabolically labelled AR42J cells in a buffer containing magnesium and ATP. This resulted in rapid dissociation of the protein of M_r 70K, showing that its interaction with PERK can be regulated by ATP and further indicating that it may belong to the HSP (heat-shock protein) 70 family of chaperones (Fig. 1b). We subjected the protein of M_r 70K to tryptic digestion within the gel and to mass spectrometry, and identified it as rat BiP (48% of the predicted tryptic fragments of BiP were present in the digest and these accounted for >50% of the peaks in the mass spectra). This identification was confirmed by immunoblotting with antisera against rodent BiP (Fig. 1c).

PERK activation during ER stress correlates with phosphorylation of its cytoplasmic kinase domain. This retards the mobility of PERK on SDS-polyacrylamide gels and serves as a convenient marker for its activation status⁸ (Fig. 2a). To examine the functional relationship between the luminal domains of IRE1 and PERK, we tested the ability of the luminal domain of IRE1 β to replace that of PERK in mediating responsiveness to ER stress. When expressed in COS-1 cells, the chimaeric IRE1 β -PERK protein, like authentic PERK, exhibited a mobility shift in response to ER stress (Fig. 2a). A similar chimaera prepared using a mutant form of PERK that lacks kinase activity (IRE1 β -PERK(K618A)) did not shift in response to ER stress. This indicates that PERK and IRE1 may respond to common luminal signals.

We examined the ability of IRE1 to associate with BiP. Mammals possess two *IRE1* genes — *IRE1 α* , which is expressed at highest levels in the pancreas⁵, and *IRE1 β* , the expression of which is restricted to epithelial cells in the gut (our unpublished observations). Antise-

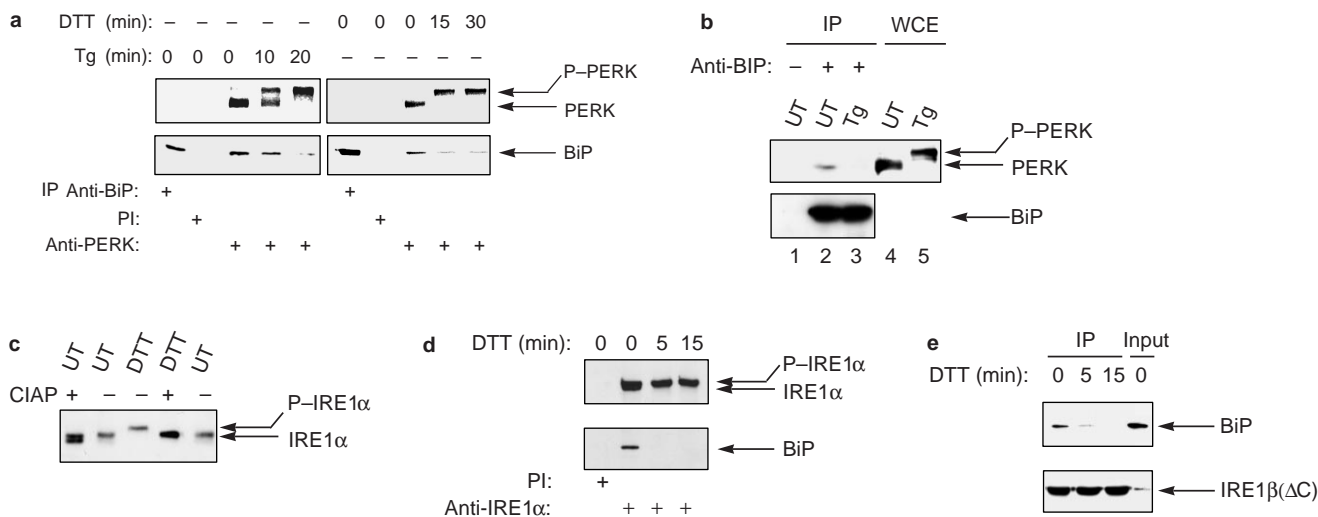


Figure 3 ER stress leads to dissociation of the BiP-PERK and BiP-IRE1 α complexes. **a**, Autoradiogram of metabolically labelled proteins from AR42J cells treated with thapsigargin (Tg) or dithiothreitol (DTT) for the indicated time periods, and immunoprecipitation with the indicated antisera. Complex components were resolved by SDS-PAGE. PI, pre-immune serum; P-PERK, phosphorylated PERK. **b**, Contents of BiP-containing complexes immunopurified from untreated (UT) or thapsigargin-treated CHO cells using a rat monoclonal antibody against hamster BiP (IP, lanes 2, 3; lane 1 represents a control). Complex components were analysed by immunoblotting against PERK (upper panel) and BiP (lower panel). Lanes 4, 5 represent whole-cell extracts (WCE) and serve to mark the migration of phosphorylated and unphosphorylated PERK. **c**, Immunoblot against IRE1 α from untreated (UT) and DTT-treated AR42J cells.

Phosphorylated (P-IRE1 α) and unphosphorylated IRE1 α were resolved by SDS-PAGE. Where indicated, immune complexes were treated *in vitro* with calf-intestine alkaline phosphatase (CIAP). **d**, Contents of IRE1 α -BiP complexes immunopurified using an antiserum against the IRE1 α C terminus from cells treated with DTT for the indicated time periods. Complex components were analysed by immunoblotting against IRE1 α (upper panel) and BiP (lower panel). **e**, Contents of complexes containing a truncated form of IRE1 β that lacks most of the C-terminal domain (IRE1 β (Δ C)). Complexes were immunopurified from NIH 3T3 cells stably expressing IRE1 β (Δ C) that were treated with DTT for the indicated time periods. Complex components were analysed by immunoblotting against BiP (upper panel) and IRE1 β (Δ C) (lower panel). The lane labelled 'input' was loaded with 1/500 of the lysate volume used in immunoprecipitation reactions.

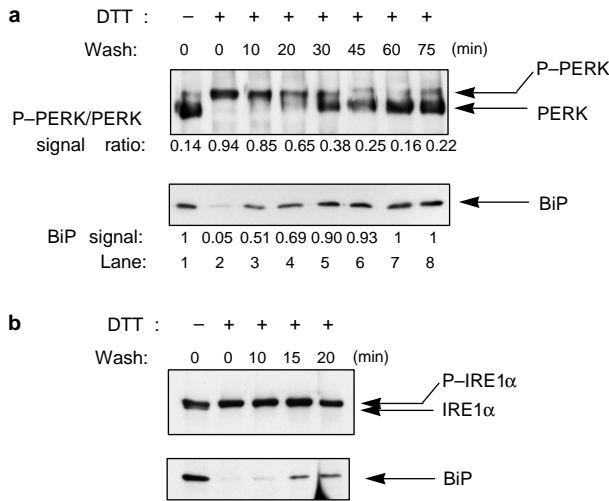


Figure 4 BiP reassociates with PERK and IRE1 α upon removal of ER stress. **a**, Dynamics of PERK–BiP complex formation, as shown by co-immunoprecipitation using anti-PERK antiserum from lysates of untreated AR42J cells and AR42J cells treated with dithiothreitol (DTT) for 15 min and then placed in DTT-free media for the indicated time periods. The ratio of the signal from phosphorylated PERK (P-PERK) to the total PERK signal, and the intensity of the BiP signal in each lane were densitometrically quantified. Note that reformation of the PERK–BiP complex precedes PERK dephosphorylation. **b**, Dynamics of IRE1 α –BiP complex formation in AR42J cells, determined as in **a** using an anti-IRE1 antiserum. Activation-dependent changes in IRE1 α mobility are not evident under the electrophoresis conditions required to resolve both IRE1 α and BiP.

rum against the C terminus of IRE1 α co-immunoprecipitated BiP from extracts of AR42J cells, whereas antiserum against IRE1 β co-immunoprecipitated BiP from extracts of mouse-stomach mucosa but not from AR42J extracts (Fig. 2b). Recovery of BiP in the immunoprecipitate therefore requires the presence of its binding partner, indicating that IRE1 and PERK may associate with BiP.

BiP associates transiently with many proteins during their synthesis and maturation¹¹. However, PERK has an estimated half-life of 13 h (Fig. 2c), and it is therefore unlikely that much of the PERK present in cells at any one time represents newly synthesized protein undergoing BiP-assisted folding. Thus, the association between PERK and BiP is unlikely to represent binding of the chaperone to nascent PERK.

Reversible dissociation of BiP complexes. We studied the PERK–BiP complex during the ER stress response. We treated AR42J cells with thapsigargin or dithiothreitol (DTT), two agents that interfere with protein folding in the ER, and examined the association between PERK and BiP by immunoprecipitating PERK from lysates of metabolically labelled cells. The quantity of BiP associated with PERK decreased within a few minutes of application of ER stress (Fig. 3a). A marked reduction was also observed in the amount of BiP associated with IRE1 α in stressed AR42J cells (Fig. 3d). Loss of BiP binding correlated with PERK and IRE1 α activation, as reflected by a shift in their mobility to more slowly migrating forms. This mobility shift was easier to detect in PERK than in IRE1 α , particularly in the 7% SDS–polyacrylamide gels used to resolve BiP (see above). In both cases, however, mobility shifts were caused by phosphorylation events, as they were readily reversed by *in vitro* treatment with alkaline phosphatase (Fig. 3c and ref. 8). DTT treatment caused a more obvious shift in IRE1 α mobility and more pronounced BiP dissociation than did thapsigargin treatment (data not shown), whereas PERK was equally responsive to both agents; the reason for this is unknown.

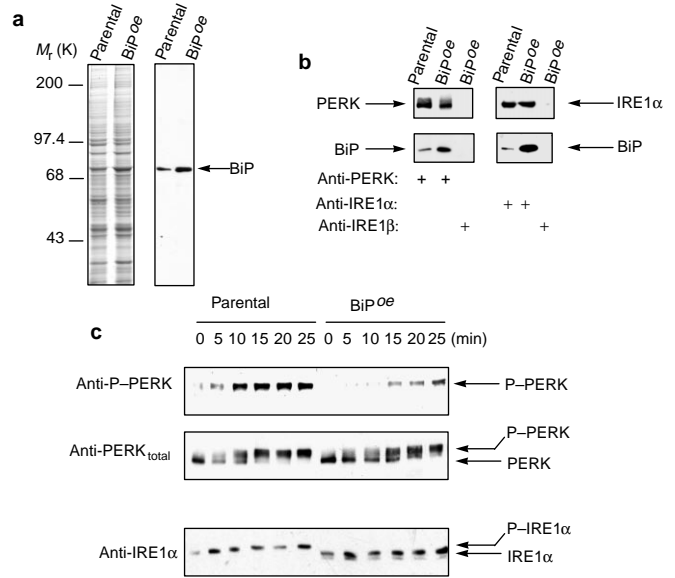


Figure 5 BiP binding and activation of stress-signal transducers in BiP-overexpressing CHO cells. **a**, Levels of BiP in whole-cell extracts from parental CHO cells and CHO cells overexpressing BiP (BiP^{oe}), as determined by SDS–PAGE with Coomassie-blue staining (left panel) and immunoblotting against BiP (right panel). **b**, Contents of PERK–BiP (left panels) and IRE1 α –BiP (right panels) complexes immunoprecipitated from parental and BiP-overexpressing CHO cells, as determined by immunoblotting with the indicated antisera. **c**, Immunoblots, after immunoprecipitation, of PERK and IRE1 α from parental and BiP-overexpressing CHO cells treated with 1 μ M thapsigargin (upper and middle panels) or 10mM DTT (lower panel) for the indicated time periods. PERK was detected using antisera against phosphorylated PERK (P-PERK; upper panel) and against all forms of PERK (PERK_{total}; middle panel); IRE1 α was detected using an antiserum against all forms of IRE1 α . Note that, in BiP-overexpressing cells, phosphorylation of PERK and IRE1 α is incomplete. A faint, faster-migrating band was revealed in BiP-overexpressing cells by IRE1 α antiserum; its significance is not known.

We were unable to detect PERK (or IRE1) in immunoprecipitates using polyclonal rabbit anti-BiP serum (Fig. 1a, c). This may be a result of the low cellular concentrations of PERK and IRE1 relative to that of BiP, or of steric hindrance of the antibody-binding site of BiP by bound PERK or IRE1. We therefore used a rat monoclonal antibody to immunoprecipitate BiP from hamster CHO-K12 cells and determined the presence of BiP-associated PERK by immunoblotting. PERK was found to be associated with BiP in unstressed cells but not in stressed cells (Fig. 3b). Furthermore, BiP-associated PERK exhibited high mobility on SDS–polyacrylamide gels, indicating that it may have been inactive (unphosphorylated). This reciprocal immunoprecipitation confirms the link between dissociation of the PERK–BiP complex and PERK activation. We were unable to detect IRE1 α in BiP-immunoprecipitation reactions, probably because of the lower level of expression of IRE1 α compared with that of PERK in CHO-K12 cells (the monoclonal antibody does not react with rat BiP and could not be used in AR42J cells, an enriched source of IRE1 α).

Signal transduction during the ER stress response is likely to be initiated on the luminal side of the ER membrane, favouring a model in which dissociation of BiP from the luminal domains of stress-signal transducers is an early upstream event leading to their phosphorylation and activation. To critically examine this hypothesis, we investigated the effect of ER stress on the association of endogenous BiP with a stably expressed, truncated version of IRE1 β , IRE1 β (Δ C)⁶, which contains the luminal and transmembrane domains but lacks most of the cytoplasmic kinase domain.

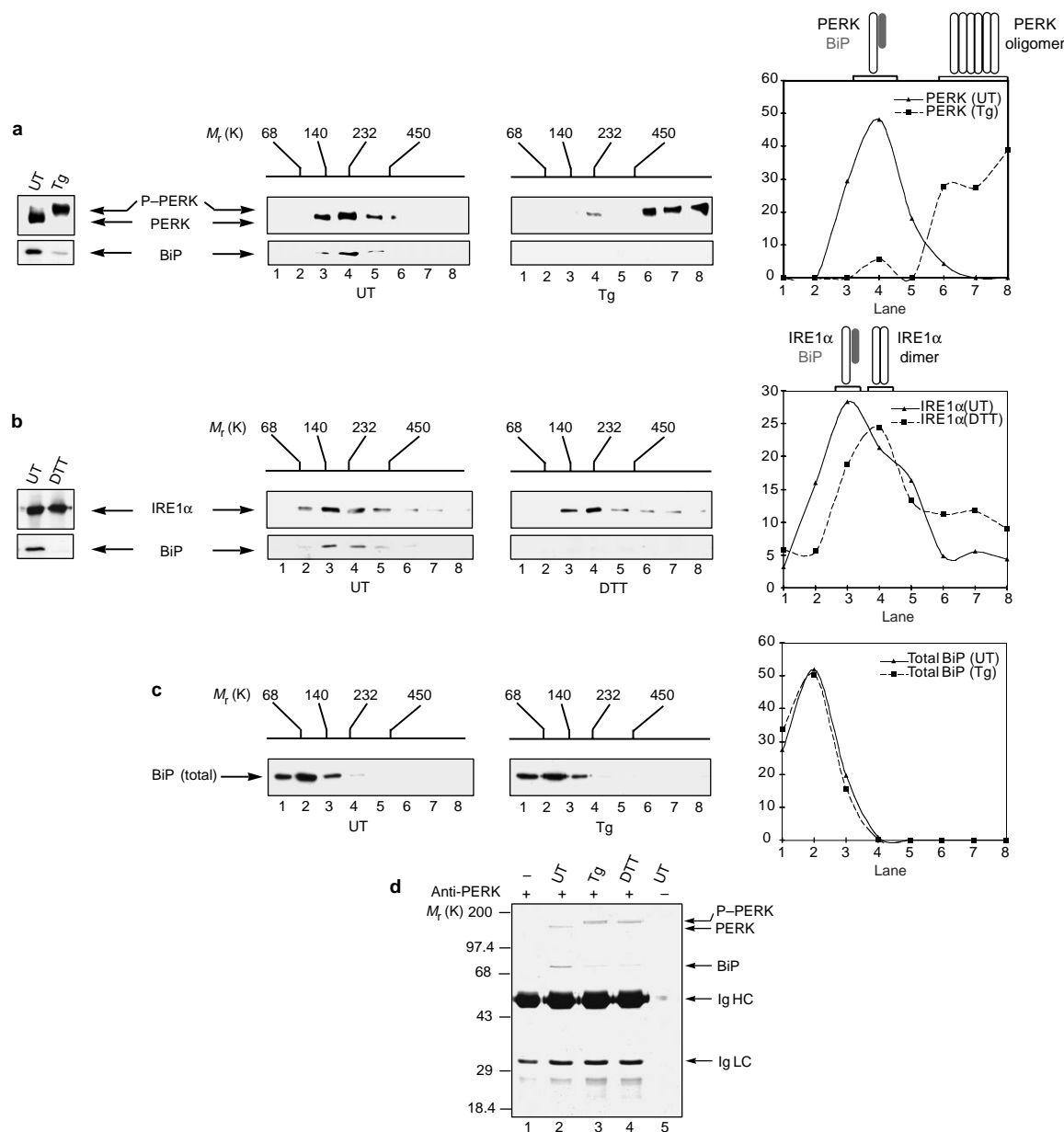


Figure 6 ER-stress-induced formation of high-molecular mass complexes containing PERK or IRE1 α but lacking BiP. **a**, Left panel, contents of PERK–BiP complexes from lysates of untreated (UT) or thapsigargin-treated (Tg; 1 μ M, 30 min) AR42J cells. Complexes were immunopurified using anti-PERK antiserum and their components identified by immunoblotting. P-PERK, phosphorylated PERK. Middle panels, analysis of complex contents as above after size fractionation of lysates by sedimentation on a 20–40% glycerol gradient. The positions of protein M_r markers, fractionated in parallel on an identical gradient, are indicated. Right panel, quantified levels of protein in size-fractionated blots. **b**, Left panel, contents of IRE1 α –BiP complexes from lysates of untreated or dithiothreitol-treated (DTT; 10 mM, 30 min) AR42J cells. Complexes were immunopurified using anti-IRE1 α antiserum and their components identified by immunoblotting. Middle panels,

analysis of complex contents after size fractionation as in **a**. Right panel, quantification of data from size-fractionated blots as in **a**. **c**, Left and middle panels, immunoblots showing the total quantity of BiP in size-fractionated lysates of untreated and thapsigargin-treated AR42J cells. Lanes were loaded with 1/1,000 of the volume used in **a**. Right panel, quantification of data from blots as in **a**, **b**, **d**. Contents of PERK-containing immune complexes isolated from untreated, thapsigargin-treated or DTT-treated AR42J cells using anti-PERK antiserum (lane 5 represents a control). Complex components were resolved by SDS-PAGE and stained with Coomassie blue. The positions of unphosphorylated and phosphorylated PERK, BiP and the immunoglobulin heavy (Ig HC) and light (Ig LC) chains are indicated. Lane 1, control containing no cell lysate.

Previous experiments using mammalian cells and yeast have shown that truncated IRE1 localizes to the ER in the same way as the wild type^{5,14}. Using NIH 3T3 cells stably expressing 9E10-tagged IRE1 β (Δ C), we immunopurified IRE1 β (Δ C)-containing complexes and determined their BiP contents by western blotting.

Treatment of cells with DTT resulted in a marked decrease in the quantity of BiP associated with the recombinant protein (Fig. 3e). Because IRE1 β (Δ C) lacks most of the C-terminal portion of IRE1 β , it is incapable of undergoing autotransphosphorylation, and is also unlikely to serve as a substrate for endogenous IRE1. Dissociation

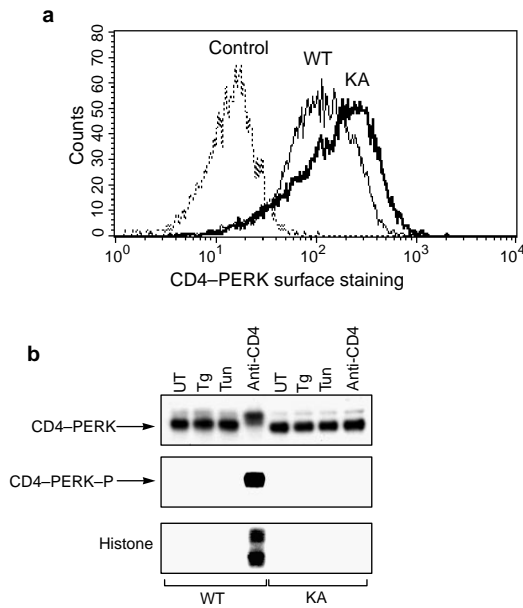


Figure 7 Oligomerization-induced activation of PERK kinase in vivo. **a**, FACS analysis of NIH 3T3 cells stably expressing fusions of the extracellular domain of CD4 with either wild-type (WT) or K618A-mutant (KA) PERK kinase domains. Untransfected cells were used as a control. Surface proteins were stained with a monoclonal anti-CD4 antibody. **b**, Upper panel, immunoblot against CD4-PERK immunoprecipitated from untreated, thapsigargin-treated (Tg; 1 μ M, 30 min), tunicamycin-treated (Tun; 2.5 μ g ml⁻¹, 4 h) or anti-CD4-antibody-treated NIH 3T3 cells. Middle and lower panels, autoradiograms showing *in vitro* PERK kinase activity after incubation with [γ -³²P]ATP. Middle panel, autophosphorylation (CD4-PERK-P, phosphorylated CD4-PERK); lower panel, phosphorylation of a histone substrate. Note the presence of two bands of differing mobility.

of the IRE1-BiP complex during ER stress therefore occurs independently of phosphorylation of the IRE1 effector domain. This result supports the idea that complex dissociation initiates signalling in the unfolded-protein response.

To examine further the dynamics of the BiP-PERK interaction, we made use of the fact that ER stress induced by DTT is readily reversible. Brief exposure to DTT was sufficient to cause dissociation of the PERK-BiP complex and activation of PERK (Fig. 4a, lane 2). However, the BiP-PERK complex rapidly reformed after DTT was washed out (Fig. 4a, lane 3). Reassociation of BiP with PERK preceded conversion of PERK from a phosphorylated, lower-mobility form to a dephosphorylated, higher-mobility form (Fig. 4a, lanes 3-8). PERK was therefore presumably still activated during reformation of the BiP-PERK complex, indicating that formation and dissociation of this complex may respond rapidly to changes in the luminal environment, and may precede changes in the activation status of the PERK effector domain. The interaction of BiP with IRE1 α exhibited similarly rapid complex reformation when DTT was washed out (Fig. 4b). These results are consistent with a function for BiP binding in determination of the activation status of ER stress-signal transducers.

CHO cells stably overexpressing BiP have a markedly attenuated unfolded-protein response^{12,13}. In these cells, the amount of chaperone associated with PERK or IRE1 α was considerably greater than in parental CHO cells expressing normal levels of endogenous BiP (Fig. 5a, b). Phosphorylation of PERK was both delayed and incomplete in BiP-overexpressing CHO cells compared with parental cells (Fig. 5c, upper and middle panels), and activation of IRE1 α by ER stress, as reflected by its shift to lower mobility on SDS-polyacrylamide gels, was absent in BiP-overexpressing cells (Fig. 5c, lower panel). These results support the idea

that overexpression of BiP attenuates ER stress signalling upstream of PERK and IRE1 activation.

Oligomerization of PERK and IRE1. It has been proposed that oligomerization has an important function in activation of ER stress-signal transducers^{14,15}. When fractionated by glycerol-gradient sedimentation, PERK from untreated cells migrated as a single peak with an apparent M_r of ~230K, which is consistent with the predicted size of a PERK-BiP heterodimer. Treatment of cells with thapsigargin (or DTT, data not shown) resulted in rapid formation of a PERK-containing complex of high M_r (estimated at >600K). The retarded mobility of this complex on SDS-polyacrylamide gels showed that its PERK was phosphorylated (Fig. 6a). BiP was readily detected in anti-PERK immunoprecipitates from the lower- M_r complex obtained from untreated cells, but was undetectable in anti-PERK immunoprecipitates obtained from the higher- M_r complex (Fig. 6a).

We examined the composition of the PERK-containing complex of M_r >600K by protein staining of the anti-PERK immunoprecipitates obtained from ER-stressed cells (Fig. 6d). The only proteins detected in these immunoprecipitates were immunoglobulin heavy and light chains, PERK and BiP; the amount of BiP was reduced during ER stress (Fig. 6d, lanes 3, 4). We carried out these immunoprecipitation reactions under conditions that preserved the integrity of the high- M_r PERK-containing complex — the same conditions that were used to prepare the glycerol gradients. The absence of other species therefore indicates that this complex may principally consist of PERK oligomers.

In untreated cells, IRE1 α was present in a complex of M_r 140K-230K, which is consistent with a subunit stoichiometry of one IRE1 α and one BiP molecule. ER stress resulted in a modest, but reproducible, shift of the IRE1 α peak to a heavier fraction. Mass estimates for the IRE1-containing peaks in the two conditions were consistent with loss of BiP binding and formation of IRE1 α homodimers during DTT treatment (Fig. 6b), and the magnitude of the DTT-induced shift in the IRE1 α peak was consistent with the small difference in mass between IRE1 α -BiP heterodimers and IRE1 α homodimers. ER stress did not affect the mobility of the majority of BiP in AR42J cells, indicating that the observed alterations in the compositions of the anti-PERK and anti-IRE1 α immunoprecipitates may reflect changes to PERK- or IRE1 α -containing complexes, rather than changes in the state of BiP (Fig. 6c).

The formation of PERK- and IRE1-containing complexes of higher M_r during the unfolded-protein response is consistent with an oligomerization step preceding transphosphorylation. PKR, an eIF2 α kinase related to PERK, is also activated by oligomerization¹⁶. To determine whether oligomerization can directly lead to PERK activation, we fused the cytoplasmic kinase domain of PERK to the extracellular and transmembrane domains of the T-lymphocyte co-receptor CD4. CD4-PERK was stably expressed on the surfaces of NIH 3T3 cells and its kinase activity was found to be dormant (Fig. 7a, b). However, we observed a marked increase in CD4-PERK kinase activity upon incubation of cells with a monoclonal antibody that crosslinks the CD4 extracellular domain¹⁷. This activation was reflected in the lower mobility, on SDS-polyacrylamide gels, of the CD4-PERK fusion protein, in its *in vitro* autokinase activity and in its kinase activity with respect to a substrate protein (Fig. 7b). We used a CD4-PERK chimaera that lacks kinase activity as a control. Thus, oligomerization is sufficient to activate the kinase activity of PERK in a heterologous location. Furthermore, the wild-type CD4-PERK chimaera was unresponsive to ER stress, indicating that PERK activation by ER stress may not be an intrinsic property of its cytosolic kinase domain, and may depend on its luminal domain.

Discussion

Although IRE1 and PERK share only weak sequence similarity in their luminal domains, our data indicate that they may use a similar mechanism to sense ER stress. We have shown that BiP binds to the

luminal domains of both of these proteins. The interactions of BiP with IRE1 and with PERK are disrupted by conditions that perturb protein folding in the ER, and are rapidly restored upon termination of stress. Activated PERK and IRE1 are found, probably as oligomers, in high- M_r complexes that lack BiP; oligomerization can induce the kinase activity of PERK even in the absence of ER stress. These findings are consistent with a model in which BiP binds to the luminal domains of PERK or IRE1 and constitutively inhibits their oligomerization. In this model, therefore, activation is dependent on a derepression step effected by release of BiP from stress-signal transducers.

This BiP release could be caused by the accumulation of misfolded proteins that compete with the luminal domains of stress-signal transducers for BiP binding. However, if the *in vivo* stability of the complexes bears any relationship to their stability *in vitro* (Fig. 1b, lane 4), the low off-rates observed would not be consistent with complex dissociation simply on the basis of competition for BiP binding by mass action. Perturbations in the ER environment could lead to modification of BiP, causing its release from stress-signal transducers; BiP would thus serve as a regulatory repressive subunit of a holoreceptor complex. The BiP component of the holoreceptor could be the target for the primary luminal event; alternatively, ER homologues of co-factors that modify the activity of the HSP70 chaperone¹⁸ may be upstream mediators in the dissociation step. Another possibility is that the luminal domains of IRE1 and PERK may be the primary recipients of the luminal signal and that their modification would result in loss of BiP binding and subsequent oligomerization of stress-signal transducers. Finally, although PERK complexes isolated from stressed cells do not contain further species detectable by protein staining (Fig. 6d), it remains possible that activation of stress-signal transducers also involves ligands that were not observed in our assay.

We have not addressed the mechanism by which BiP retains bound stress-signal transducers in inactive forms. It is possible that BiP binds to a single high-affinity site, thereby masking a domain that is essential for oligomerization. Alternatively, BiP may bind to several sites in the luminal domain, interfering with oligomerization in a manner that is biochemically less specific and stochastic. A precedent for BiP binding, with low sequence specificity, to several segments of a polypeptide was recently provided by analysis of the function of BiP in post-translational translocation of proteins into the yeast ER¹⁹. The estimated size of the PERK–BiP and IRE1–BiP complex from non-stressed AR42J cells is consistent with a stoichiometric ratio of 1:1 (Fig. 6a, b). However, PERK and IRE1 α immunopurified from BiP-overexpressing CHO cells were associated with many BiP molecules (Fig. 5b). This may be because of the presence of several potential BiP-binding sites in the luminal domains of stress transducers that are revealed when BiP is overexpressed. It also possible, however, that BiP binds to a single site on the transducers, but can do so as an oligomer, which would account for the unusual stoichiometry of transducer–BiP complexes in BiP-overexpressing cells.

Our findings support a model that is similar to the negative-feedback mechanism by which heat-shock proteins control their own expression. Under normal conditions in *Escherichia coli*, the σ 32 subunit of RNA polymerase, which is specific to the heat-shock promoter, is engaged in an inactive complex by the HSP70-like BiP homologue DNAK^{20,21}. Accumulation of misfolded proteins releases σ 32 from its inactive complex with DNAK, thereby increasing transcription from heat-shock promoters²². A conceptually similar mechanism applies to the constitutive repression of mammalian heat-shock transcription factor HSF by HSPs. Heat shock leads to loss of HSP binding, HSF trimerization, promoter binding and activation of HSP-encoding genes^{23,24}. Thus, in examples from several phyla and from different cellular compartments, overexpression of HSPs attenuates stress responses^{12,13,22,25}. Our findings indicate that, in the mammalian ER, this may be because of the ability of BiP to repress the activity of ER stress-signal transducers. We thus provide a missing link in the model, originally proposed over seven years ago²⁶, to explain a key function of BiP in ER stress signalling. □

Methods

Antibodies.

Rabbit polyclonal antisera were directed against the C-terminal 507 residues of mouse IRE1 α , the C-terminal 516 residues of mouse IRE1 β and residues 588–1,024 of mouse GCN2. Antisera against total PERK were directed against a bacterially expressed protein fragment lacking kinase activity (the C-terminal 417 residues of mouse PERK). Antiserum against phosphorylated PERK was directed against a peptide fragment (the C-terminal 501 residues of mouse PERK) that is heavily autophosphorylated⁸. Specific antibodies against phosphorylated PERK were obtained by depleting the anti-phospho-PERK antiserum against a protein identical to the immunogen except for a mutation, K618A, that inactivated its kinase domain and rendered the protein unable to undergo autophosphorylation⁸. Antibodies against mouse CD4 were produced as a tissue culture supernatant of the GK1.5 rat anti-mouse-CD4 hybridoma cell line (ATCC). Polyclonal rabbit and monoclonal rat anti-BiP immunochromatals were as described^{27,28}.

Expression plasmids and transfections.

The IRE1 β –PERK plasmid encoded the amino-terminal 499 residues of mouse IRE1 β , encompassing the luminal and transmembrane domains, and the cytoplasmic C-terminal kinase domain of mouse PERK (residues 537–1,114); its expression was driven by the viral promoter in the pBABE.puro plasmid. The CD4–PERK plasmid encoded the extracellular and transmembrane domains of mouse CD4 (residues 1–396) and the cytoplasmic domain of mouse PERK; its expression was driven by the viral promoter described above. COS-1 cells were transfected in 6-cm dishes with 3 μ g of the indicated expression plasmid, using the DEAE–dextran method. Protein extracts were prepared 36h later in 50 μ l 1% Triton buffer (20mM HEPES pH7.5, 150mM NaCl, 1% Triton X-100, 10% glycerol, 1mM EDTA, 10mM tetrasodium pyrophosphate, 100mM NaF, 17.5mM B-glycerophosphate, 1mM phenylmethylsulphonyl fluoride (PMSF), 4mg ml⁻¹ aprotinin and 2mg ml⁻¹ pepstatin A); 10 μ l of each extract were analysed by immunoblotting against PERK, as described below.

NIH 3T3 cell lines stably expressing CD4–PERK were prepared by retroviral infection and selection with puromycin. Individual colonies were isolated and screened by immunoblotting for expression of CD4–PERK. Surface expression of the fusion protein was confirmed by FACS analysis of cells ($n = 5 \times 10^5$) stained with a 1/10 dilution of GK1.5 culture supernatant, followed by washing and incubation with a 1/50 dilution of phycoerythrin-labelled goat anti-rat antibody (Caltag, Burlingame, California, USA).

Induction of ER stress, immunoprecipitation and immunoblotting.

Dishes of 10-cm diameter containing confluent AR42J cells, CHO-K12 cells, BiP-overexpressing CHO cells or CD4–PERK-expressing NIH 3T3 cells were either left untreated or treated with 2.5 μ g ml⁻¹ tunicamycin, 10mM DTT or 1 μ M thapsigargin or with a 1:10 dilution (v/v) of GK1.5 hybridoma culture supernatant, for 30 min or as indicated in (Figs 3–7). Plates were washed in ice-cold PBS containing 1mM EDTA, lysed in 200 μ l 1% Triton buffer (see above) and clarified by centrifugation at 16,000g for 10 min and by preincubation for 1h with 10 μ l protein–A–sepharose. Soluble proteins were immunoprecipitated with 1 μ l of the anti-PERK or anti-IRE1 polyclonal antisera bound to 10 μ l protein–A–sepharose and washed three times in RIPA buffer; bound proteins were resolved by 7% SDS–PAGE under reducing conditions and transferred to nitrocellulose membranes. Blots were incubated with rabbit anti-PERK antibody (10,000 dilution) or antisera against IRE1 α (1/2,000), IRE1 β (1/2,000), BiP (1/1,000), ribophorin 1 (1/1,000) or GCN2 (1/1,000); signals were observed using protein A tagged with horseradish peroxidase (1/5,000) and enhanced chemiluminescence. For Coomassie-blue staining of immunopurified protein complexes from AR42J cells in ten plates of 10-cm diameter, 3 μ l of polyclonal antibodies (Fig. 1a) or 4 μ g of affinity-purified anti-PERK antibody (Fig. 5d) were used. Immunoprecipitation–kinase assays were carried out at 30 °C for 30 min, in a 20- μ l reaction volume containing washed immunoprecipitated proteins attached to protein–A–sepharose beads in kinase buffer (20mM HEPES pH7.5, 50mM KCl, 2mM magnesium acetate, 2mM MnCl₂, 1.5mM DTT and 2.5mM ATP) supplemented with 5 μ Ci [γ -³²P]ATP (4,500 Ci mmol⁻¹; ICN). Where indicated (Fig. 7b), 5 μ g of calf thymus histone mix (Sigma) were added to the reaction.

Metabolic labelling.

AR42J cells at 70% confluence in 6-cm dishes were starved for 30 min in methionine/cysteine-free media, pulse-labelled with 500 μ Ci [³⁵S]Met–Cys express-labelling mix (ICN) for 30 min, and then cold-chased in complete media for the indicated time periods (Fig. 2c) or for 20h (Figs 1a, 3a). This long chase was required to completely reverse the induction of the unfolded-protein response that took place when cells were deprived of methionine. Extracts and immunoprecipitations were carried out as described above; labelled protein complexes were resolved by SDS–PAGE and observed using autoradiography.

Glycerol-gradient sedimentation.

Confluent AR42J cells in 10-cm dishes were lysed in 300 μ l 1% Triton buffer (see above). Extracts or high- M_r markers (Pharmacia) were centrifuged through 20–40% glycerol gradients in polyallomer tubes of 11 \times 60 mm as described²⁹. Each 4-ml gradient was divided into eight equal fractions of 500 μ l. Aliquots of each fraction (0.5 μ l) were subjected to SDS–PAGE; the BiP content was measured by immunoblotting. The contents of PERK- and IRE1 α -containing complexes were analysed, after adjustment of the glycerol concentration in each fraction to 20%, by sequential immunoprecipitation and immunoblotting using anti-PERK or anti-IRE1 α antisera as described above.

RECEIVED 10 DECEMBER 1999; REVISED 21 FEBRUARY 2000; ACCEPTED 1 APRIL 2000; PUBLISHED 8 MAY 2000.

- Lee, A. Mammalian stress response: induction of the glucose-regulated protein family. *Curr. Biol.* 4, 267–273 (1992).
- Brostrom, C. O. & Brostrom, M. A. Regulation of translational initiation during cellular responses to stress. *Prog. Nucleic Acid Res. Mol. Biol.* 58, 79–125 (1998).
- Chapman, R., Sidrauski, C. & Walter, P. Intracellular signaling from the endoplasmic reticulum to the nucleus. *Annu. Rev. Cell Dev. Biol.* 14, 459–485 (1998).
- Kaufman, R. J. Stress signaling from the lumen of the endoplasmic reticulum: coordination of gene transcriptional and translational controls. *Genes Dev.* 13, 1211–1233 (1999).
- Tirasophon, W., Welihinda, A. A. & Kaufman, R. J. A stress response pathway from the endoplasmic reticulum to the nucleus requires a novel bifunctional protein kinase/endoribonuclease (Ire1p) in mammalian cells. *Genes Dev.* 12, 1812–1824 (1998).

6. Wang, X. Z. *et al.* Cloning of mammalian Ire1 reveals diversity in the ER stress responses. *EMBO J.* **17**, 5708–5717 (1998).
7. Shi, Y. *et al.* Identification and characterization of pancreatic eukaryotic initiation factor 2 alpha-subunit kinase, PEK, involved in translational control. *Mol. Cell Biol.* **18**, 7499–7509 (1998).
8. Harding, H., Zhang, Y. & Ron, D. Translation and protein folding are coupled by an endoplasmic reticulum resident kinase. *Nature* **397**, 271–274 (1999).
9. Munro, S. & Pelham, H. R. An Hsp70-like protein in the ER: identity with the 78 kDa glucose-regulated protein and immunoglobulin heavy chain binding protein. *Cell* **46**, 291–300 (1986).
10. Wei, J. & Hendershot, L. M. Characterization of the nucleotide binding properties and ATPase activity of recombinant hamster BiP purified from bacteria. *J. Biol. Chem.* **270**, 26670–26676 (1995).
11. Hebert, D. N., Simons, J. F., Peterson, J. R. & Helenius, A. Calnexin, calreticulin, and Bip/Kar2p in protein folding. *Cold Spring Harb. Symp. Quant. Biol.* **60**, 405–415 (1995).
12. Dorner, A., Wasley, L. & Kaufman, R. Overexpression of GRP78 mitigates stress induction of glucose regulated proteins and blocks secretion of selective proteins in Chinese hamster ovary cells. *EMBO J.* **11**, 1563–1571 (1992).
13. Wang, X-Z. *et al.* Signals from the stressed endoplasmic reticulum induce C/EBP homologous protein (CHOP/GADD153). *Mol. Cell Biol.* **16**, 4273–4280 (1996).
14. Shamu, C. E. & Walter, P. Oligomerization and phosphorylation of the Ire1p kinase during intracellular signaling from the endoplasmic reticulum to the nucleus. *EMBO J.* **15**, 3028–3039 (1996).
15. Welihinda, A. A. & Kaufman, R. J. The unfolded protein response pathway in *Saccharomyces cerevisiae*. Oligomerization and *trans*-phosphorylation of Ire1p (Ern1p) are required for kinase activation. *J. Biol. Chem.* **271**, 18181–18187 (1996).
16. Langland, J. O. & Jacobs, B. L. Cytosolic double-stranded RNA-dependent protein kinase is likely a dimer of partially phosphorylated M_r 66,000 subunits. *J. Biol. Chem.* **267**, 10729–10736 (1992).
17. Reinhard, C., Shamon, B., Shyamala, V. & Williams, L. T. Tumor necrosis factor alpha-induced activation of c-jun N-terminal kinase is mediated by TRAF2. *EMBO J.* **16**, 1080–1092 (1997).
18. Bukau, B. & Horwich, A. L. The Hsp70 and Hsp60 chaperone machines. *Cell* **92**, 351–366 (1998).
19. Matlack, K. E., Misselwitz, B., Plath, K. & Rapoport, T. A. BiP acts as a molecular ratchet during posttranslational transport of prepro-alpha factor across the ER membrane. *Cell* **97**, 553–564 (1999).
20. Liberek, K., Galitski, T. P., Zylitz, M. & Georgopoulos, C. The DnaK chaperone modulates the heat shock response of *Escherichia coli* by binding to the sigma 32 transcription factor. *Proc. Natl Acad. Sci. USA* **89**, 3516–3520 (1992).
21. Gamer, J., Bujard, H. & Bukau, B. Physical interaction between heat shock proteins DnaK, DnaJ, and GrpE and the bacterial heat shock transcription factor sigma 32. *Cell* **69**, 833–842 (1992).
22. Tomoyasu, T., Ogura, T., Tatsuta, T. & Bukau, B. Levels of DnaK and DnaJ provide tight control of heat shock gene expression and protein repair in *Escherichia coli*. *Mol. Microbiol.* **30**, 567–581 (1998).
23. Morimoto, R. I. Regulation of the heat shock transcriptional response: cross talk between a family of heat shock factors, molecular chaperones, and negative regulators. *Genes Dev.* **12**, 3788–3796 (1998).
24. Zou, J., Guo, Y., Guettouche, T., Smith, D. F. & Voellmy, R. Repression of heat shock transcription factor HSF1 activation by HSP90 (HSP90 complex) that forms a stress-sensitive complex with HSF1. *Cell* **94**, 471–480 (1998).
25. Straus, D. B., Walter, W. A. & Gross, C. A. The activity of sigma 32 is reduced under conditions of excess heat shock protein production in *Escherichia coli*. *Genes Dev.* **3**, 2003–2010 (1989).
26. Kohno, K., Normington, K., Sambrook, J., Gething, M. J. & Mori, K. The promoter region of the yeast KAR2 (BiP) gene contains a regulatory domain that responds to the presence of unfolded proteins in the endoplasmic reticulum. *Mol. Cell Biol.* **13**, 877–890 (1993).
27. Freiden, P. J., Gaut, J. R. & Hendershot, L. M. Interconversion of three differentially modified and assembled forms of BiP. *EMBO J.* **11**, 63–70 (1992).
28. Hendershot, L. M. *et al.* *In vivo* expression of mammalian BiP ATPase mutants causes disruption of the endoplasmic reticulum. *Mol. Biol. Cell* **6**, 283–296 (1995).
29. Bertolotti, A. *et al.* EWS, but not EWS-FLI-1, is associated with both TFIID and RNA polymerase II: interactions between two members of the TET family, EWS and hTAFII68, and subunits of TFIID and RNA polymerase II complexes. *Mol. Cell Biol.* **18**, 1489–1497 (1998).

ACKNOWLEDGEMENTS

We thank G. Kreibich for the anti-ribophorin antiserum, D. Littman for CD4 cDNA and monoclonal antibody, R. Kaufman and A. Dorner for CHO.BiP⁺ cells, M. A. Gawinowicz for mass spectroscopy and J-P. Simon for help with glycerol gradients. This work was supported by NIH grants (ES08681 and DK47119) to D.R., National Research Service award (NRSA) to H.P.H. and EMBO and Human Frontier Science programme awards to A.B. D.R. is a Stephen Birnbaum Scholar of the Leukaemia Society of America.

Correspondence and requests for materials should be addressed to D.R.